applied sciences

MDPI

Article

Acoustics of Compressed Earth Blocks Bound Using Sugarcane Bagasse Ash and Water Hyacinth Ash

Nicholas O. Ongwen [1,2] and Adel Bandar Alruqi [3,*]

[1] Department of Physics and Materials Science, Maseno University, Maseno 40137, Kenya; apache.nc.22@gmail.com
[2] Faculty of Biological and Physical Sciences, Tom Mboya University, Homa-Bay 40300, Kenya
[3] Department of Physics, Faculty of Science, King Abdulaziz University, Jeddah 21589, Saudi Arabia
* Correspondence: aalruqi@kau.edu.sa

Abstract: Mechanical compaction is often used to densify building earth blocks by reducing the void between the particles. Compacted stabilised earth involves a binder, which holds the particles of the materials together. The compaction and addition of binders to the earth can modify its transport, mechanical, and acoustical properties. In this study, the acoustic transmission coefficient, porosity, and airflow resistivity were investigated by varying the concentrations of water hyacinth ash (WHA) and sugarcane bagasse ash (SBA) binders. An acoustic test rig comprising an acoustic wave guide made from joined water pipes was employed to analyse the influence of the WHA and SBA binders on the acoustical performance of the earth blocks. It was found out that the measured acoustic wave transmission was sensitive to the variation in the composition of WHA and SBA in the earth blocks. Increasing the WHA concentration led to an increase in the acoustic transmission coefficient and porosity, but reduced the airflow resistivity of the compressed earth blocks; while increasing the SBA reduced the transmission coefficient and porosity, but increased the airflow resistivity. This shows that SBA has a stronger binding property than WHA, which is ideal for the manufacture of stronger earth blocks, while the higher porosity of the earth blocks obtained with WHA is good for the construction of porous walls, which is good for maintaining the airflow between the inside of buildings and the surrounding.

Keywords: earth blocks; micropolar behaviour; sugarcane bagasse ash; water hyacinth ash; acoustical properties of compressed earth blocks

Citation: Ongwen, N.O.; Alruqi, A.B. Acoustics of Compressed Earth Blocks Bound Using Sugarcane Bagasse Ash and Water Hyacinth Ash. *Appl. Sci.* **2023**, *13*, 8223. https://doi.org/10.3390/app13148223

Academic Editors: Muamer Kadic and Gino Iannace

Received: 7 June 2023
Revised: 29 June 2023
Accepted: 12 July 2023
Published: 15 July 2023

1. Introduction

Concrete is today the building material that is most commonly used worldwide. It is basically a combination of sand and cement, with the cement acting as a binder that glues the sand particles together. However, cement is not only expensive, but its production leads to emission of acidic carbon IV oxide into the atmosphere, which is one of the main greenhouse gases that can lead to global warming. Among the alternatives to cement that have been explored include geopolymer concrete, which has been found to be suitable in addition to being environmentally friendly. Moreover, the geopolymer has been found to process higher strength and deformation properties due to its more stable and denser aluminosilicate spatial microstructure [1–5]. Sand, on the other hand, is not always readily available, and can be expensive to purchase and transport, especially for people living in areas that are far away from where sand is found. Sand mining/harvesting is also one of the major causes of erosion of coastlines [6].

Earth (soil) is a natural material and is readily available on construction sites, in addition to being cheap and environmentally friendly. It has thus been utilised in the construction of walls of houses, more so in the developing countries. The simplest form of houses made of earth is called mud houses, whose walls (rammed earth walls) are simply

constructed by mixing earth (a mixture of aggregates that include gravel, sand, silt, and a small amount of clay) and water, and then using this mixture to fill the spaces between flat panels, usually called formwork [7]. Earth building is a renewable and sustainable technology, and has become the means of providing safe, comfortable, and desirable homes [8]. However, the recent generation has developed negative views about earth-built houses, associating them with rural poverty, lack of exposure, and backwardness [9].

One of the main shortcomings of mud houses is their short lifespan. Normal earthen houses are unable to withstand harsh tropical rainy seasons. This is because the earthen walls soon start to develop cracks, which usually occurs because the earth particles are not sufficiently held together due to poor binding, as well as very low compaction pressure. However, a lot of research has been ongoing over the recent decades into the modifications of the earth blocks so as to improve their properties. These include altering the compaction pressure, as well as making them interlocking. The roughness of these walls has also undergone modifications, with the aim of making the walls smooth and thus, providing aesthetic value [10–12]. Figure 1 shows some of the modern earth blocks with aesthetic value, as well as better mechanical properties that are currently being used in the construction of walls of houses.

Figure 1. Modern earth blocks used in the construction of walls of houses (images taken from houses under construction in Busia Country, Kenya).

In the search for alternative binders to cement, many materials have been investigated, including fly ash, rice husk, silica fume, eggshell, groundnut shell, sugarcane bagasse ash, cassava powder, waste glass, coal bottom ash, waste marble powder, and waste-derived ceramic concrete [13–23]. However, large quantities of these materials that can be used in building reasonable-sized houses may not be easy to find. Water hyacinth (*Eichhornia crassipes*) is an aquatic plant that is a nuisance. It causes many problems, including loss of biodiversity, water loss, effects on water quality, damage to infrastructure, and poor health of aquatic species. The hyacinth is freely available and is in large quantities in water bodies (freshwater lakes). Thus, finding its use in the construction of earth blocks serves as a way of utilising it. In the past, it has been used to make concrete in order to increase the material's permeability and tensile strength [24], as well as the partial replacement of cement in the form of water hyacinth ash (WHA) [16]. WHA consists mainly of calcium oxide (22.61%), potassium oxide (14.82%), magnesium oxide (14.01%), and silica (4.40%), with a specific gravity of 2.44. According to a study by Murugesh, Balasundaram, and Vadivel [25], using WHA in place of some of the cement decreases corrosion and weakens the concrete's resistance to chloride erosion.

Sugarcane bagasse is a waste product that comes out of the sugar manufacturing industries. It is a fibrous waste that is obtained after sugarcane juice has been squeezed out of the sugarcane. If not well managed, it can cause environmental pollution and thus, finding ways of recycling it can help to solve the environmental pollution caused by such agricultural waste [26–30]. However, these wastes have an advantage over other waste materials in that they are renewable. Sugarcane bagasse contains about 50% cellulose,

25% hemicellulose, and 25% lignin [31]. When burnt, the sugarcane bagasse forms ash (sugarcane bagasse ash, SBA), which contains traces of metals such as silver, arsenic, barium, chromium, gold, and lead [32]. The chemical composition of WHA has been investigated, where its main components have been found to include silica (64.88%), alumina (6.40%), calcium oxide (10.69%), and iron III oxide (2.63%), with a specific gravity of 2.20. Of these, silica, alumina, and iron III oxide, which should contribute at least 70%, are the contributors to the pozzolanic reactions [33].

The acoustical characterisation of compressed earth blocks has been explored, including the works by Mansour et al. [34] and Mansour et al. [35], who investigated the effect of compaction pressure on porosity, airflow resistivity, tortuosity, and viscous characteristic length. The studies found out that addition of both compaction pressure and cement led to a decrease in the porosity and a corresponding increase in the airflow resistivity of the CEBs. However, these two studies considered only cement as the binder to the soil. In a recent study by Ouma et al. [36], the acoustics (acoustic transmission coefficient, porosity, and airflow resistivity) of WHA and lime were explored. This study therefore did not consider SBA as a binder to the earth. A study by Butko, Holliday, and Reyes [37] also explored the sound intensity that was transmitted through walls constructed using CEBs in comparison to wood-framed walls. The study found out that the CEB walls were better than the wood-framed walls in that they reduced the noise by half and, therefore, provided more isolation between the interior and exterior acoustic sources. In this work, the influence of varying the binder type (WHA and SBA) and their concentrations on acoustical properties (acoustic transmission coefficient, porosity, and airflow resistivity) were studied. The porosity and airflow resistivity were determined using the equivalent fluid model (EFM) by solving an inverse acoustic problem [38]. This study's specific objectives were (i) to determine the impact of WHA content on the acoustical properties (acoustic transmission coefficient, porosity, and airflow resistivity) of compressed earth blocks (CEBs) and (ii) to determine the impact of SBA content on the acoustical properties (acoustic transmission coefficient, porosity, and airflow resistivity) of CEBs.

2. Materials and Methods

2.1. Sample Preparation

The main raw materials used in this study were earth, WHA, and SBA. These materials were chosen since they are readily available and cheap. The earth was obtained locally in Busia County, Mayenje Ward, Kenya. The earth from this region has been praised for its value in making high-quality earth blocks. Following one month of storage at room temperature with a relative humidity of 63% and shaded storage, the collected earth samples were broken down and made suitable for use by passing them through a 0.2 mm sieve in order to remove the large particles. The water hyacinth was taken from Lake Victoria near Kisumu, Kenya. After being collected, the hyacinth sample was cleaned and washed in water in order to remove dirt and other contaminants. The sample was then uniformly divided into 2 cm long pieces, which were subsequently sun-dried for two weeks. After being dried, the sample was baked for 10 h at 230 °C in order to convert the organic material into an inorganic substance, after which it was milled. The duration and the temperature were ideal for the conversation. The ground sample was then run through an 8 mm sieve in order to obtain a fine powder. Sugarcane bagasse was obtained from a local sugar factory (Kibos Sugar Factory, Kisumu, Kenya). The obtained bagasse was then dried in the open air for one week, after which it was burnt in the air in order to obtain the SBA. Figure 2 shows the prepared raw materials. The choice of the sample mixture was informed by that of a previous study [35], where earth was replaced with cement of up to 15%.

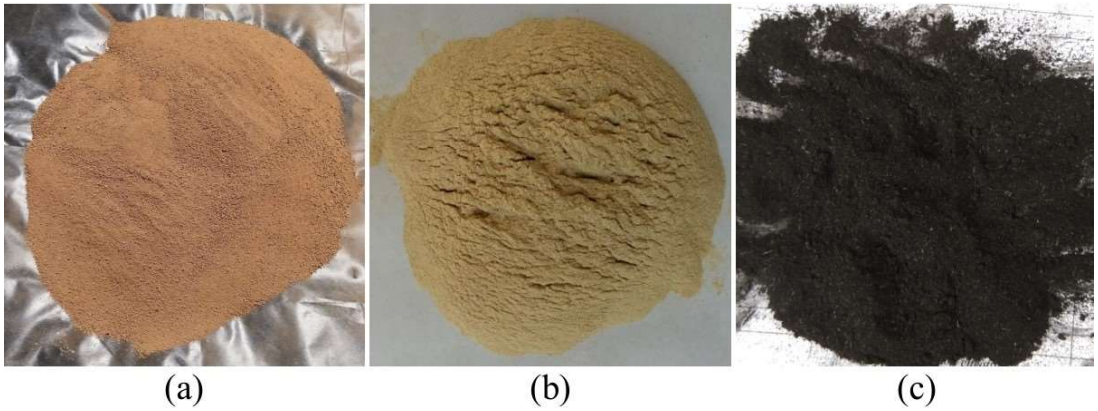

Figure 2. The prepared raw materials, ready for use in making the earth blocks: (**a**) Earth; (**b**) Water hyacinth ash; (**c**) Sugarcane bagasse ash.

The three raw materials (earth, WHA, and SBA) were then weighed using the Mettler Toledo PB303 (Mettler Toledo, Zürich, Switzerland) with an analytical balance of accuracy at 0.001 g and a maximum weighing capacity of 310 g, after which they were mechanically mixed at different ratios (Table 1). Following the addition of water, the mixturing continued until the mixture became homogenous. In preparing the sample CEBs, a sample holder was used. The sample holder was a cylindrical metal sheet with an internal diameter of 76.2 mm and a thickness of 20 mm. The choice of the measurement of the internal diameter was guided by the internal diameter of the acoustic waveguide where the CEB samples were placed when making the acoustic transmission measurements.

Table 1. The different percentages by mass (in grams) of earth, water hyacinth ash, sugarcane bagasse ash, and water. They are given sample identities SG1–SG8.

Sample ID	Soil	WHA	SBA	Water (mL)
SG1	100	0.0	0.0	60
SG2	95	5.0	0.0	90
SG3	90	10.0	0.0	160
SG4	85	15.0	0.0	170
SG5	85	12.0	3.0	110
SG6	85	10.0	5.0	100
SG7	85	7.0	8.0	120
SG8	85	4.0	11.0	90

With the help of a nearby welder, the mould was created. The mould is displayed in Figure 3a. By employing a hydraulic press (Hydraform, model number M7TWIND, South Africa), the CEBs were created. The prepared cylindrical mould was placed inside the cuboid mould of the Hydroform, which is usually used for making standard-sized CEBs. The prepared mixture was then placed into the mould (Figure 3b) and then pressed to a pressure of 25 bars. Although increasing the compaction pressure increases the density and mechanical properties of CEBs, extremely high compaction pressure values are not good for the acoustical properties of the blocks because they reduce porosity, which results in a poor signal-to-noise ratio. Following the compaction, the CEBs were kept at an ambient temperature and relative humidity of 60% for 14 days. The sample identifiers (SG1–SG8) were assigned to the CEB samples. Figure 3d shows some of the prepared CEB samples that had already been removed from the mould, whereas Figure 3c shows the prepared CEB samples still inside the mould.

Figure 3. (**a**) The cylindrical metallic mould for making the compressed earth block samples; (**b**) The mould placed inside the normal brick mould; (**c**) The wet compressed earth block that was still inside the cylindrical mould; (**d**) Some of the prepared compressed earth block samples.

2.2. Measurements

We decided to calculate the CEB samples' transmission coefficients. This was due to the direct relationship between the transmission coefficient and airflow, a mechanism that influences the loss of sound energy. The prepared CEBs samples, which were further characterised, were designed to perfectly fit into a segment of an 18.0 m long pipe (acoustic waveguide) with an internal diameter of 76.2 mm (3.00 inch), which was made up of three polyurethane water pipes connected together. The frequency range of the pipe (18.8 to 2621.6 Hz) was determined from the Formula (1) [39]:

$$f_L = \frac{v}{l + 1.6r}; \; f_H = \frac{1.8412v}{2\pi r} \tag{1}$$

where v is the sound velocity of the air used as the fluid in this work, l is the total length of the pipe, r is the radius of the waveguide, f_L is the lower threshold frequency of the pipe, and f_H is the higher threshold frequency. By extending the pipe, it was possible to reduce the lower frequency limit even more. However, this was dependent on how much empty space there was in the testing area.

A speaker-driven ribbon tweeter was fixed to the waveguide through a metallic cylindrical tube, with one end flattened and holes made, which were later used to fix the loudspeaker with bolts and nuts, while the other end had an external diameter of 76.2 mm (same as the internal diameter of the waveguide), such that it fits exactly into the waveguide. Rubber was then wrapped around the joint so as to minimise acoustic leakage (Figure 4a–c). Before feeding the signal into the loudspeaker, it was amplified using an amplifier removed from a sub-woofer. An omnidirectional microphone (ABM-716-RC Pro-Signal, Farnell, Leeds, England) was used to record the incident and transmit acoustic waves in order to record the loudspeaker's signals. It was positioned downstream of the pipe. Figure 4c shows the microphone being fixed onto the waveguide using black tape. This microphone was inserted into the waveguide at a distance of 9 m from the loudspeaker. The microphone was operated by a 9 V heavy-duty battery. The loudspeaker then produced sound waves in the pipe, which was joined to a signal generator (a Thurlby Thandar TG 210 generator made in the UK). The intended output of the generator was a Heaviside signal (step function). Putty (brand and address) was used to stop the leakage of waves that occurred between the margins of the samples and the walls of the waveguide as a result of the samples' imperfect circularity.

Finally, a digital oscilloscope (picoscope 4262, Cambridgeshire, UK) was attached to the microphone. This oscilloscope has a frequency limit of 5 MHz, with a 16 bits-bit rate. The signal from the microphone was fed to channel 1, while the signal from the signal generator was fed to channel 2 of the picoscope. Figure 5 shows the scheme of the experimental setup.

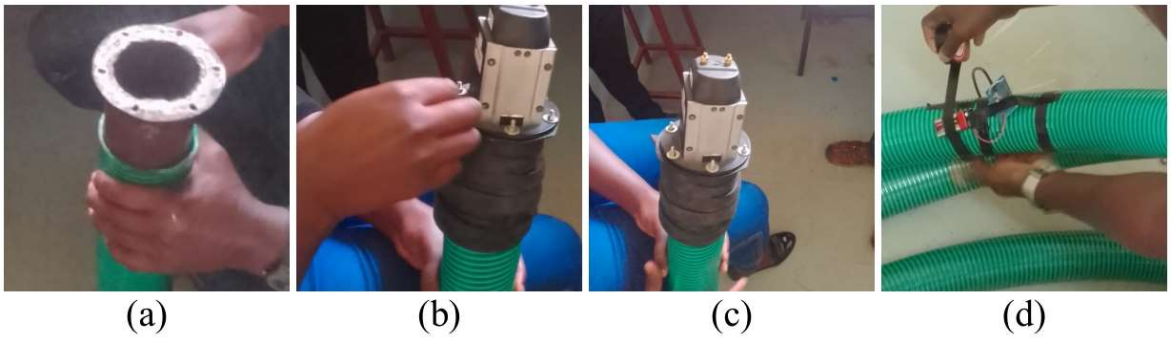

Figure 4. (**a**) Fixing the loudspeaker support to the pipe; (**b**) Making the combination airtight using butyl rubber; (**c**) The mounted loudspeaker-waveguide setup; and (**d**) Fixing the microphone to the waveguide.

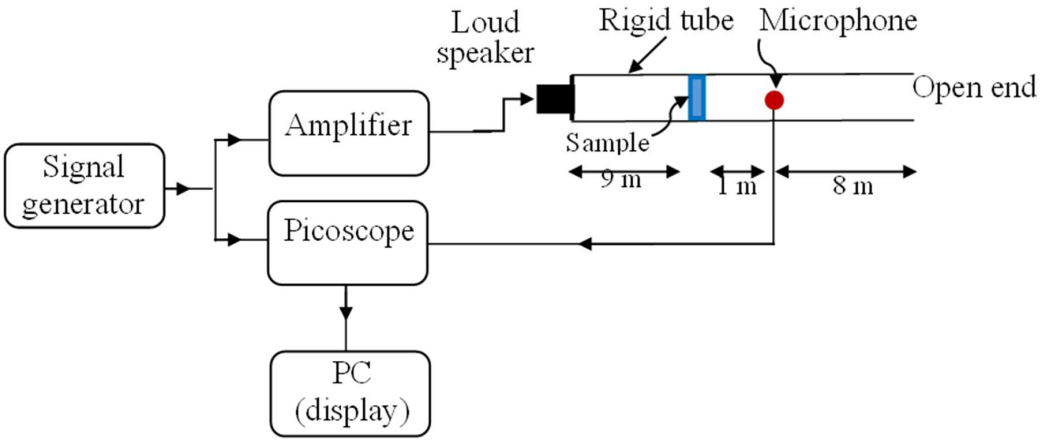

Figure 5. The experimental set up for the measurement of the incident and transmitted sound signals through the sample.

The signal with and without the sample were both recorded. The acoustic waveguide's overall length was set to be sufficient to prevent a time overlap between the transmitted acoustic waves moving downstream and those reflected from the open end. The microphone's placement was carefully considered to ensure that the reflected waves were placed at a distance from the transmitted ones. A personal computer (PC) was then used to visualise these response signals. The duration of the temporal window in which the recorded transmitted pressure wave signals were digitalised was determined in order to eliminate the reflected waves from the open end of the waveguide. The transmission coefficient was calculated from this incident (without the sample) and transmitted (with the sample) signals using the transfer function. According to Ogam et al. [40], the transfer function T(f) was calculated by dividing the power spectral density S_I of the $p_I(t)$ and the cross power spectral density S_T of the incident $p_I(t)$ and transmitted $p_T(t)$ acoustic pressure:

$$T(f) = \frac{S_T(f)}{S_I(f)} \tag{2}$$

An inverse problem was then solved in order to extract the two acoustical properties (porosity and airflow resistivity) from the measured transmission coefficient (Equation (2)) of a porous slab in a long waveguide using an EFM and an acoustic/CEB interaction model of the acoustic wave transmission. Since air, a light fluid, saturated the porous CEB materials, the EFM approximation was applied. For each set of trial values for the parameter, a functional error was generated that reflected the distinction between the transmission coefficient data from the interaction model (IM) and from the experimental one. The cost functional $\Im$ expressing this discrepancy was chosen as:

$$\Im\left(\omega,\ \phi,\ \sigma,\ \Lambda,\ \alpha_\infty,\ k_o',\ \frac{\Lambda\prime}{\Lambda}\right) = \sum_{n=1}^{N_s}\left[\left|T^{EFM}\left(\omega,\ \phi,\ \sigma,\ \Lambda,\ \alpha_\infty,\ k_o',\ \frac{\Lambda\prime}{\Lambda}\right)\right| - |T^{exp}(\omega)|\right]^2 \quad (3)$$

where T^{exp} T is the transmission coefficient gleaned from the waveguide. The cost functional $\Im$ was minimized in order to obtain the parameters. By changing the model parameters at various, reasonably close intervals, the minimum of this cost functional was achieved [41]. The tortuosity ranged from 1.0 to 3.0, whereas the porosity ranged from 0.1 to 1.0. When $\Im$ displayed a parabolic form, the global minima of the cost functionals were obtained as the solution for each parameter. The two sought-after parameters were converged using a manual iterative method that was performed for each parameter at a time [42]. The objective functional curves for each parameter were plotted against the two parameters that were sought.

3. Results and Discussion

3.1. Transmission Coefficient

Figure 6 displays the eight samples' transmission coefficients, as determined by Equation (2). Figure 6a–d demonstrates that adding WHA to the earth enhanced the microstructural acoustical properties like porosity, a result that was crucial for the construction of walls and allowed internal air to flow out through the walls and, thus, reduce the concentration of indoor air pollutants. The transmission coefficient was observed to increase with increase in the WHA content, as can be shown in Figure 6a–d. This is in agreement with a previous study by Ouma et al. [36], who also observed the increase in the transmission coefficient with an increase in the WHA content. However, SBA was found to reduce the transmission coefficient (Figure 6e–h). This is also in accordance with a previous study by Chusilp, Jaturapitakkul, and Kiattikomol [33], which showed that SBA is very rich in silica content (64.88% silica), unlike WHA, which contains only 4.40% [26]. The silica (Cementous material) in the SBA binder reacted with portlandite (calcium hydroxide) to form an additional calcium silicate hydrate gel. For pozzolan, the sum of the composition of silica, alumina, and iron III oxide should be more than 70%, a condition that has been met by SBA in previous studies but has not been met by WHA. In fact, the study by Chusilp, Jaturapitakkul, and Kiattikomol [33] found this value to be 73.91% for SBA. This explains why SBA-bound CEBs in this study showed stronger binding compared to the WHA-bound CEBs and thus, lower transmission coefficients. A lower transmission coefficient implies a lower intensity, which leads to a reduction in the sound between the inside and the outside of a house, a phenomenon that is ideal for occupants that live near noisy places such as those located close to airports.

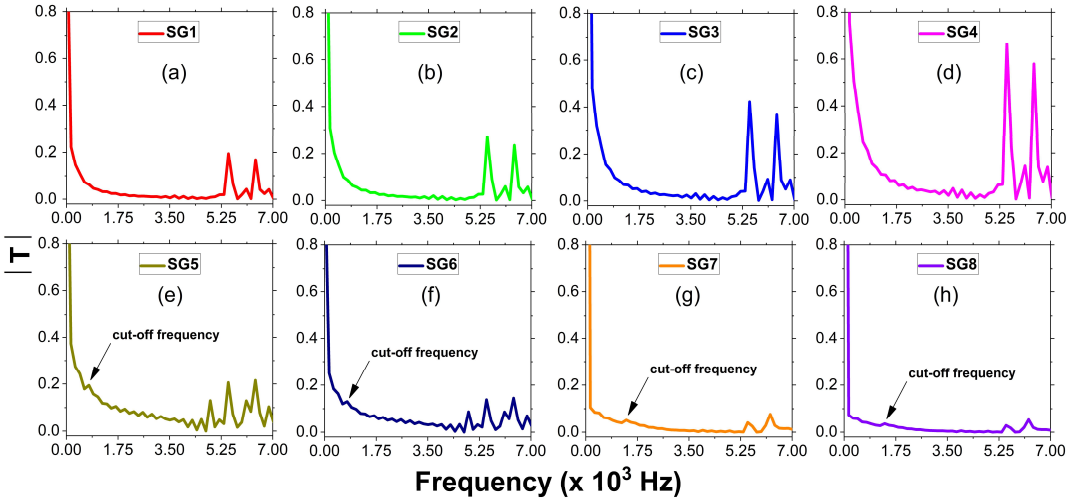

Figure 6. Transmission coefficients of the 8 samples of the earth blocks (SG1 to SG8): (**a**–**d**) CEBs bound using WHA, and (**e**–**h**) CEBs bound using SBA.

3.2. Inversion of the Transmission Coefficient Data Using the EFM Interaction Model

Figure 7 shows the minima of the cost function with porosity for all eight CEB samples. From the minima, the values of the porosity were determined, which are presented in Table 2. In order to evaluate the performance of the model and the pertinence of the recovered parameters, a reconstructed transmission coefficient was used with the interaction model and the experimental data (Figure 6). The porosity consistently increased as the WHA increased (samples SG1 to SG4), which is in accordance with the finding by Ouma et al. [36]. This could be explained by the fact that an increase in the WHA content causes the CEBs to become void-filled, which lowers their resistance to the airflow through CEBs. This study's results on porosity indicate that manufactured CEBs are generally porous, particularly at high WHA concentrations. Therefore, they are appropriate for building porous walls. The SBA, on the other hand, was found to lower the porosity, which is in line with its effect in lowering the transmission coefficient, since a more porous material can transmit more sound and vice versa. However, not much information is available in the literature on the acoustics of CEBs when bound using SBA. This study thus forms a basis for future reference.

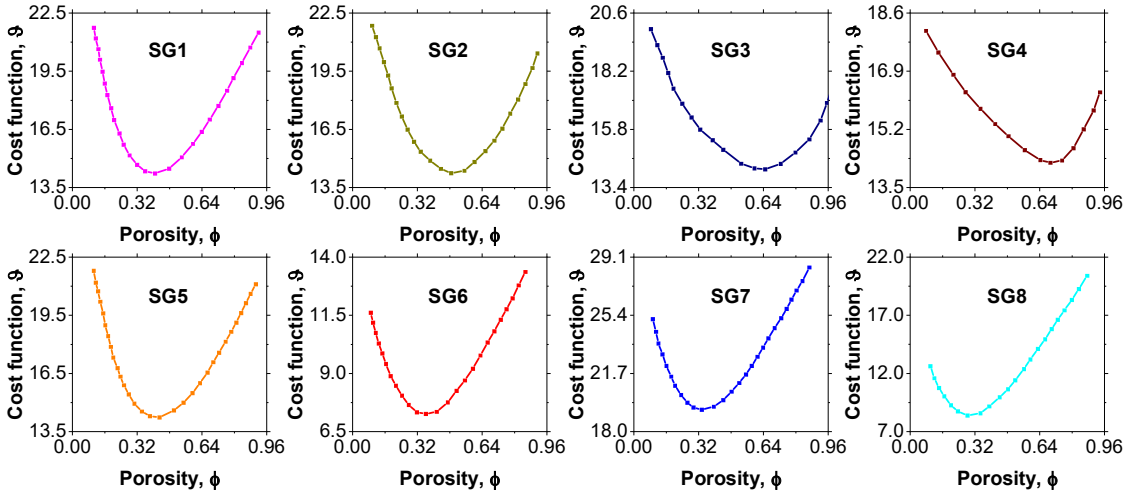

Figure 7. Cost function against porosity for all the eight compressed earth block samples.

Table 2. The calculated porosity and airflow resistivity for all the eight compressed earth block samples.

Sample	SG1	SG2	SG3	SG4	SG5	SG6	SG7	SG8
Φ	0.40	0.51	0.64	0.70	0.42	0.37	0.34	0.29
σ ($\times 10^3$ pa·s·m^{-2})	11.8	9.2	7.5	6.0	11.0	13.8	17.8	22.2

Table 2 shows that the porosities of the CEB samples manufactured in this study were sensitive to the concentration of the binders, with the CEBs bound using WHA (SG1 to SG4) demonstrating higher values of the porosity compared to those bound using SBA (SG5 to SG8). This finding is very consistent with the finding for the transmission coefficients (Figure 6a–d).

The variation in the airflow resistivity with the WHA and SBA concentration can be observed in Figure 8. As the concentration of WHA (SG1 to SG4) increased, it was found that the airflow resistivity reduced continuously, which is pretty compatible with the rise in porosity, given that the two were inversely connected. The airflow resistivity was observed to rise steadily as the concentration of SBA (SG5 to SG8) increased, which was also consistent with the decline in the porosity. Because WHA increased the number of voids in the CEB samples, it lessened the proximity of the particles, which is why the airflow resistivity decreased as the WHA concentration increased. This increased the samples' resistance to sound passing through them. By contrast, the closeness of the particles

increased by more strongly binding them together as the concentration of SBA increased, which lowers the voids in the CEB samples. This increased the samples' resistance to sound passing through it. Table 2 displays the computed values for the airflow resistivity.

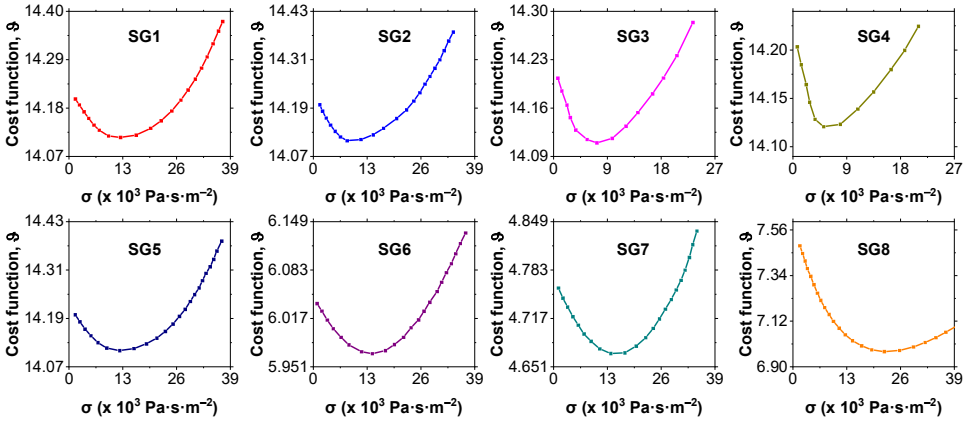

Figure 8. Cost function against airflow resistivity for all the eight compressed earth block samples.

4. Conclusions

To determine the transmission coefficients of CEBs with different percentages of earth, WHA, and SBA, a straightforward acoustic test apparatus was constructed by utilizing water pipes to create a long acoustic waveguide. It was established that the blocks' measured acoustic transmission coefficients were sensitive enough to pick up on the small percentage fluctuations in their composition. This made it possible to comprehend the impact that each binder and its quantity had on the acoustical properties. It was determined that the two binders exhibited different behaviors. While SBA reduced the transmission coefficient and porosity (from 0.42 to 0.29 when the SBA was increased from 0% to 11%) and increased airflow resistivity (from 11.0 $\times$ 10^3 pa·s·m^{-2} to 22.2 $\times$ 10^3 pa·s·m^{-2}), the WHA was shown to increase the transmission coefficient and porosity (from 0.4 to 0.7 when the WHA was increased from 0% to 15%) and reduce airflow resistivity (from 11.8 $\times$ 10^3 pa·s·m^{-2} to 6.0 $\times$ 10^3 pa·s·m^{-2}). The WHA and SBA-bound CEBs investigated in this study were found to be generally porous and, therefore, ideal for the construction of porous walls. The lowering of the transmission coefficient by SBA is highly desired for building houses that are located in noisy places, such as those close to airports or railway lines. However, the mechanical properties, which equally play a crucial role in the confection of building materials, were not considered for these CEBs. Studies therefore need to be conducted on the mechanical properties of the blocks.

Author Contributions: Conceptualization, N.O.O. and A.B.A.; methodology, N.O.O.; software, N.O.O.; validation, N.O.O.; formal analysis, N.O.O. and A.B.A.; investigation, N.O.O. and A.B.A.; resources; N.O.O. and A.B.A.; data curation, N.O.O.; writing—original draft preparation, N.O.O. and A.B.A.; writing—review and editing, N.O.O. and A.B.A. All authors have read and agreed to the published version of the manuscript.

Funding: This research work was funded by Institutional Fund Projects under grant no. (IFPIP: 1142-130-1443). The authors gratefully acknowledge technical and financial support provided by the Ministry of Education and King Abdulaziz University, DSR, Jeddah, Saudi Arabia.

Institutional Review Board Statement: Not applicable.

Informed Consent Statement: Not applicable.

Data Availability Statement: Data sharing is not applicable to this article.

Conflicts of Interest: The authors declare no conflict of interest.

References

1. Meskhi, B.; Beskopylny, A.N.; Stel'makh, S.A.; Shcherban', E.M.; Mailyan, L.R.; Shilov, A.A.; El'shaeva, D.; Shilova, K.; Karalar, M.; Aksoylu, C.; et al. Analytical review of geopolymer concrete: Retrospective and current issues. *Materials* **2023**, *16*, 3792. [CrossRef] [PubMed]
2. Acar, M.C.; Çelik, A.I.; Kayabaşı, R.; Şener, S.; Özdöner, N.; Özkılıç, Y.O. Production of perlite-based-aerated geopolymer using hydrogen peroxide as eco-friendly material for energy-efficient buildings. *J. Mater.* **2023**, *24*, 81–99. [CrossRef]
3. Çelik, A.I.; Özkılıç, Y.O. Geopolymer concrete with high strength, workability and setting time using recycled steel wires and basalt powder. *Steel Compos. Struct.* **2023**, *46*, 689. [CrossRef]
4. Çelik, A.I.; Tunç, U.; Bahrami, A.; Karalar, M.; Mydin, A.O.; Alomayri, T.; Özkılıç, Y.O. Use of waste glass powder toward more sustainable geopolymer concrete. *J. Mater.* **2023**, *24*, 8533–8546. [CrossRef]
5. Özkılıç, Y.O.; Çelik, A.I.; Tunç, U.; Karalar, M.; Deifalla, A. The use of crushed recycled glass for alkali activated fly ash based geopolymer concrete and prediction of its capacity. *J. Mater.* **2023**, *24*, 8267–8281. [CrossRef]
6. Heger, M.P.; Vashold, L.; Hentschel, J. Managing Maghreb's Eroding Coasts for Future Generations. 2021. Available online: https://www.worldbank.org/en/news/feature/2021/10/29/managing-maghreb-s-eroding-coasts-for-future-generations (accessed on 29 October 2021).
7. Minke, G. *Building with Earth: Design and Technology for a Sustainable Architecture*; Birkhauser Architecture: Basel, Switzerland, 2009.
8. Earth Building Association of Australia. 2019. Available online: https://www.ebaa.asn.au/ (accessed on 28 July 2021).
9. Marsh, A.T.; Kulshreshtha, Y. The state of earthen housing worldwide: How development affects attitudes and adoption. *Build.* **2021**, *50*, 485–501. [CrossRef]
10. Namango, S. Development of Cost-Effective Earthen Building Material for Housing Wall Construction. Doctoral Dissertation, Moi University, Cheptiret, Kenya, 2006. Available online: https://www.researchgate.net/publication/283068265 (accessed on 13 August 2006).
11. Donkor, P.; Obonyo, E. Earthen construction materials: Assessing the feasibility of improving strength and deformability of compressed earth blocks using polypropylene fibers. *Mater. Des.* **2015**, *83*, 813–819. [CrossRef]
12. Nshimiyimana, P.; Sore, S.O.; Hema, C.; Zoungrana, O.; Messan, A.; Courard, L. A discussion of "optimisation of compressed earth blocks (CEBs) using natural origin materials: A systematic literature review". *Constr. Build. Mater.* **2022**, *325*, 126887. [CrossRef]
13. Lindh, P.; Lemenkova, P. Effects of GGBS and fly ash in binders on soil stabilization for road construction. *Rom. J. Transp. Infrastruct.* **2022**, *11*, 1–13. [CrossRef]
14. Abdullah, H.; Shahin, M.; Walske, M.L. Review of fly-ash-based geopolymers for soil stabilisation with special reference to clay. *Geosciences* **2020**, *10*, 249. [CrossRef]
15. McCarthy, M.J.; Dhir, R.K. Towards maximising the use of fly ash as a binder. *Fuel* **1999**, *78*, 121–132. [CrossRef]
16. Murugesh, V.; Balasundaram, N. Experimental investigation on water hyacinth ash as the partial replacement of cement in concrete. *Int. J. Civ. Eng. Technol.* **2017**, *8*, 1013–1018.
17. Lima, S.A.; Varum, H.; Sales, A.; Neto, V.F. Analysis of the mechanical properties of compressed earth block masonry using the sugarcane bagasse ash. *Constr. Build. Mater.* **2012**, *35*, 829–837. [CrossRef]
18. Zeybek, O.; Özkılıç, Y.O.; Karalar, M.; Çelik, A.I.; Qaidi, S.; Ahmad, J.; Burduhos-Nergis, D.D.; Burduhos-Nergis, D.P. Influence of replacing cement with waste glass on mechanical properties of concrete. *Materials* **2022**, *15*, 7513. [CrossRef] [PubMed]
19. Karalar, M.; Bilir, T.; Çavuşlu, M.; Özkılıç, Y.O.; Sabri, M.M.S. Use of recycled coal bottom ash in reinforced concrete beams as replacement for aggregate. *Front. Mater.* **2022**, *9*, 1064604. [CrossRef]
20. Qaidi, S.; Najm, H.M.; Abed, S.M.; Özkılıç, Y.O.; Dughaishi, H.A.; Alosta, M.; Sabri, M.M.S.; Alkhatib, F.; Milad, A. Concrete containing waste glass as an environmentally friendly aggregate: A review on fresh and mechanical characteristics. *Materials* **2022**, *15*, 6222. [CrossRef] [PubMed]
21. Çelik, A.I.; Özkılıç, Y.O.; Zeybek, O.; Karalar, M.; Qaidi, S.; Ahmad, J.; Burduhos-Nergis, D.D.; Bejinariu, C. Mechanical behaviour of crushed waste glass as replacement of aggregates. *Materials* **2022**, *15*, 8093. [CrossRef]
22. Karalar, M.; Özkılıç, Y.O.; Aksoylu, C.; Sabri, M.M.S.; Beskopylny, A.N.; Stel'makh, S.A.; Shcherban', E.M. Flexural behaviour of reinforced concrete beams using waste marble powder towards application of sustainable concrete. *Front. Mater.* **2022**, *9*, 1068791. [CrossRef]
23. Chang, Q.; Liu, L.; Farooqi, M.U.; Thomas, B.; Özkılıç, Y.O. Data-driven based estimation of waste-derived ceramic concrete from experimental results with its environmental assessment. *J. Mater.* **2023**, *24*, 6348–6368. [CrossRef]
24. Boban, J.M.; Nair, P.V.; Shiji, S.T.; Cherian, S.E. Incorporation of water hyacinth in concrete. *Int. J. Eng. Res. Technol.* **2017**, *6*, 540–544.
25. Murugesh, V.; Balasundaram, N.; Vadivel, T.S. Experimental studies on durability studies of concrete with partial replacement of cement by water hyacinth ash. *Int. J. Eng. Technol.* **2018**, *7*, 22–24. [CrossRef]
26. Beskopylny, A.N.; Shcherban', E.M.; Stel'makh, S.A.; Meskhi, B.; Shilov, A.A.; Varavka, V.; Evtushenko, A.; Özkılıç, Y.O.; Aksoylu, C.; Karalar, M. Composition component influence on concrete properties with the additive of rubber tree seed shells. *Appl. Sci.* **2022**, *12*, 11744. [CrossRef]

27. Shcherban', E.M.; Stel'makh, S.A.; Beskopylny, A.N.; Mailyan, L.R.; Meskhi, B.; Shilov, A.A.; Chernil'nik, A.; Özkılıç, Y.O.; Aksoylu, C. Normal-weight concrete with improved stress–strain characteristics reinforced with dispersed coconut fibers. *Appl. Sci.* **2022**, *12*, 11734. [CrossRef]
28. Qaidi, S.; Al-Kamaki, Y.; Hakeem, I.; Dulaimi, A.F.; Özkılıç, Y.; Sabri, M.; Sergeev, V. Investigation of the physical-mechanical properties and durability of high-strength concrete with recycled PET as a partial replacement for fine aggregates. *Front. Mater.* **2023**, *10*, 1101146. [CrossRef]
29. Basaran, B.; Kalkan, I.; Aksoylu, C.; Özkılıç, Y.O.; Sabri, M.M.S. Effects of waste powder, fine and coarse marble aggregates on concrete compressive strength. *Sustainability* **2022**, *14*, 14388. [CrossRef]
30. Fayed, S.; Madenci, E.; Özkiliç, Y.O.; Mansour, W. Improving bond performance of ribbed steel bars embedded in recycled aggregate concrete using steel mesh fabric confinement. *Constr. build. Mater.* **2023**, *369*, 130452. [CrossRef]
31. Manikandan, A.T.; Moganraj, M. Consolidation and rebound characteristics of expansive soil by using lime and bagasse ash. *Int. J. Res. Eng. Technol.* **2014**, *3*, 403–411.
32. Faria, K.C.P.; Gurgel, R.F.; Holanda, J.N.F. Recycling of sugarcane bagasse ash waste in the production of clay bricks. *J. Environ. Manag.* **2012**, *101*, 7–12. [CrossRef]
33. Chusilp, N.; Jaturapitakkul, C.; Kiattikomol, K. Utilization of bagasse ash as a pozzolanic material in concrete. *Constr. build. Mater.* **2009**, *23*, 3352–3358. [CrossRef]
34. Mansour, M.B.; Ogam, E.; Jelidi, A.; Cherif, A.S.; Jabrallah, S.B. Influence of compaction pressure on the mechanical and acoustic properties of compacted earth blocks: An inverse multi-parameter acoustic problem. *Appl. Acoust.* **2017**, *125*, 128–135. [CrossRef]
35. Mansour, M.B.; Ogam, E.; Fellah, Z.E.A.; Cherif, A.S.; Jelidi, A.; Jabrallah, S.B. Characterization of compressed earth blocks using low frequency guided acoustic waves. *J. Acoust.* **2018**, *139*, 2551–2560. [CrossRef] [PubMed]
36. Ouma, J.; Ongwen, N.; Ogam, E.; Auma, M.; Fellah, Z.; Mageto, M.; Ben Mansour, M.; Oduor, A. Acoustical properties of compressed earth blocks: Effect of compaction pressure, water hyacinth ash and lime. *Case Stud.* **2023**, *18*, e01828. [CrossRef]
37. Butko, D.; Holliday, L.; Reyes, M. Comparing the acoustical nature of a compressed earth block (ceb) residence to a wood-framed residence. *Proc. Mtgs. Acoust.* **2014**, *22*, 015002. [CrossRef]
38. Johnson, D.L.; Koplik, J.; Dashen, R. Theory of dynamic permeability and tortuosity in fluid-saturated porous media. *J. Fluid Mech.* **1987**, *176*, 379–402. [CrossRef]
39. Ogam, E.; Fellah, Z.E.A.; Ogam, G.; Ongwen, N.O.; Oduor, A.O. Investigation of long acoustic waveguides for the very low frequency characterization of monolayer and stratified air-saturated poroelastic materials. *Appl. Acoust.* **2021**, *182*, 108200. [CrossRef]
40. Ogam, E.; Fellah, Z.E.A.; Fellah, M.; Depollier, C. Theoretical and experimental study of micropolar elastic materials using acoustic waves in air. *J. Sound Vib.* **2021**, *510*, 116298. [CrossRef]
41. Wirgin, A. Retrieval of the equivalent acoustic constitutive parameters of an inhomogeneous fluid-like object by nonlinear full waveform inversion. *Ultrasonics* **2016**, *65*, 353–369. [CrossRef]
42. Lefeuve-Mesgouez, G.; Mesgouez, A.; Ogam, E.; Scotti, T.; Wirgin, A. Retrieval of the physical properties of anelastic solid half space from seismic data. *J. Appl. Geophys.* **2013**, *88*, 70–82. [CrossRef]